

International Journal of Modern Physics B
© World Scientific Publishing Company

New Possibilities for Obtaining a Steep Nonlinear Current–Voltage Characteristics in some Semiconductor Structures

D. I. Sheka

National Taras Shevchenko University of Kyiv, Kyiv, Ukraine

O. V. Tretyak

*National Taras Shevchenko University of Kyiv, Kyiv, Ukraine
tov@univ.kiev.ua*

A. M. Korol

*Department of Physics, National University for Food Technologies, Kyiv, Ukraine
korolam@nuft.edu.ua*

A. K. Sen

*TCMP Divn, Saha Institute of Nuclear Physics, 1/AF Bidhan Nagar, Kolkata 700064, India
asokk.sen@saha.ac.in*

A. Mookerjee

*S.N. Bose National Centre for Basic Sciences, 3/JD Salt Lake, Kolkata 700098, India
abhijit@boson.bose.res.in*

Received October 24, 2018

Electronic processes in a semiconductor system consisting of some Resonant Tunnelling Structures, built in the depletion region of a Schottky barrier, are investigated. It is shown that the Schottky barrier can block or unblock the resonant tunnelling current effectively. Tunnelling processes do reveal the coherent character. Sharp nonlinear current-voltage characteristics are observed on both of the forward and the reverse branches.

1. Introduction

A lot of various resonant tunnelling structures (RTS) are being investigated widely now. Interesting results have been obtained with the use of RTS's in combination with other semiconductor structures. In this paper, we consider a combination of two structures — a resonant tunnelling structure and a Schottky barrier (SB). Such a proposal for embedding a RTS inside the decay or depletion region of a barrier may be found in the literature. It may be noted that it is not too demanding for the fabrication processes, as well. Such a barrier is often used as a convenient instrument for studying the characteristics of various electrical systems, including different types of RTS's. North et al. [1] have studied the effects associated with

the electron reflection at the semiconductor-metal interface of a Schottky collector. Resonant-tunnelling spectroscopy of quantum dots has been performed in some works, e.g., Refs. [2, 3]. Besides, the SB's may be used for other purposes, as well. For example, the effect of replacing the usual collector of a standard double barrier resonant tunnelling diode (DBRTD) by a Schottky layer has been studied [4, 5]. It was shown in these works that this could improve the frequency characteristics of the RTS's. In the case considered in this paper, however, the presence of the SB plays a fundamentally more important role in the electronic processes under study. In keeping with the current practice in studying device physics, the quantum mechanical phase of the carrier wave function and the thermal (phonon) broadening of the resonances have not been considered in the calculations below, on the assumption that their effects are small enough.

We have shown that an SB may work like a blocking barrier for the resonant tunnelling current in a system consisting of a metal and a semiconductor with a double-barrier RTS (DBRTS) placed in the space-charge (or, the depletion) region. As a result, in some cases one may observe a very sharp (jump-like) increase, and in some other cases, a similarly sharp jump-like decrease in the total current through the structure. Thus, we would like to point out that, besides the usual drop in current that is inherent in such a structure [3], we focus our attention here to the additional possibility of realizing a steep nonlinearity in its current-voltage characteristics (IVC). It should be clear from what follows that, depending on the parameters of the problem, the indicated nonlinearity may be manifested in both the forward and the reverse branches of the IVC. Thus, the SB plays here a role akin to a regulator of the electronic processes in the structure and, in particular, it influences the observed shape of the $I - V$ curves.

We choose a symmetric double-barrier RTS as the tunnelling structure, and insert it in the depletion region of a Schottky contact. In the sequel, we refer to this as a RTSC (Resonant Tunnelling Schottky Contact). The choice of the double-barrier structure is not fundamental. What is important is that only the following conditions be met: (i) the RTS chosen must have at least one resonance level (E_r) to serve as a channel for the current flow, and (ii) the size of the RTS must be considerably smaller than the width of the Schottky layer. Then the magnitude of the $I - V$ response of the RTS must depend substantially on its starting parameters, e.g., the supposed position of the resonance level E_r in relation to the top of the SB at the zero voltage bias U ; $\phi(x = 0, U = 0) \equiv \phi_0$ (see Fig. 1). If $E_r - \phi_0 > 0$ and $U = 0$, then the difference between the indicated levels increases monotonically, and the IVC has the usual exponentially increasing form. A qualitatively different situation arises when $E_r - \phi_0 < 0$ and $U = 0$. In that case, the resonance channel for the current flow (that of the RTS) is initially blocked by the SB; and the current is governed by the non-resonant tunnelling of electrons and the flow component above the barrier. As U is increased, the difference $|E_r(U) - \phi(x = 0, U)|$ decreases, and at a certain voltage $U = U_c$, a turning of the resonant channel of current passage occurs. This turning-on of the channel is accompanied by an exceedingly sharp rise of the

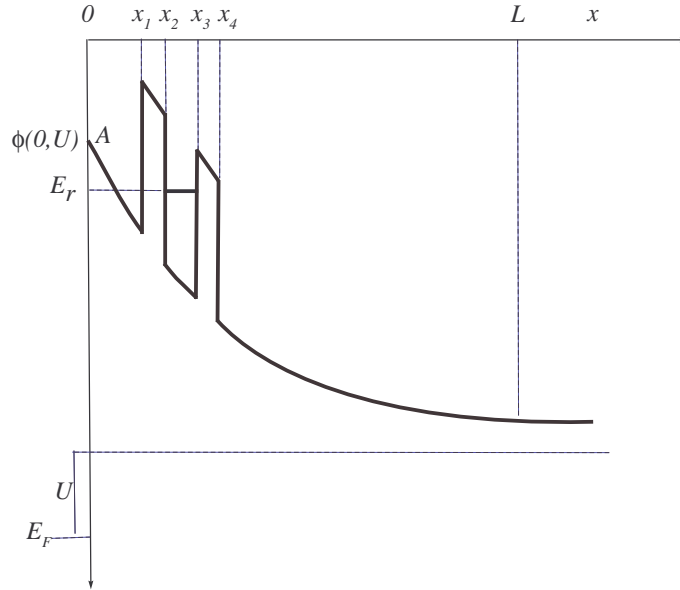


Fig. 1. The potential profile of a RTSC.

current, and that is reflected in the shape of the IVC. Thus, there is a substantial difference in the functioning of a standard DBRTS and the system considered here. In the standard system, which is initially (i.e., for $U = 0$) a symmetric structure, it is fundamentally impossible to have the conditions for a resonant tunnelling current. But, the RTSC is an asymmetric structure under an external voltage (e.g., $U > 0$) and a tunnelling current arises naturally.

We point out some additional differences reflected in the IVC between a standard DBRTS and the structure investigated here. First, the collector and the emitter regions function somewhat differently. For example, in a standard DBRTS, the collector plays the role of a reservoir capable of accepting electrons with any energy (which come from the emitter). In a RTSC (under a forward bias, $U > 0$), the emitter is a bulk semiconductor region, while the collector is the contact electrode, which can receive only an energy-restricted fraction of the electrons due to the existence of the Schottky barrier. Next, one notes that the main electron emission in a standard DBRTS takes place in the energy interval $[0, E_F]$. But, in the RTSC structure, electrons driven at high energies (due to the external field) reach the collector. Thus, the *working* energy interval corresponds, in a certain comparative sense, to *hot* electrons. Ultimately, these differences give rise to some interesting features in the IVC of the resonant tunnelling structures.

The main goal of this paper is to demonstrate the possibility of obtaining some extraordinarily steep IVC in a modern semiconductor structure. So, for simplicity, we have omitted from our considerations, such factors as the accumulation of charge

(Coulomb effects), roughness of the surface, non-parabolicity of the dispersion relation, etc., which should not influence the effect under study in a qualitative way. We should also point out that the results obtained in this study are valid in cases when the resonant tunnelling current exceeds the forward tunnelling current and the current at energies above the barrier. Our comparison of these currents shows that the stated condition is well satisfied for a wide spectrum of parameters of the problem. We calculate the current density with the formula, normally used for structures such as the RTSC's, namely,

$$j = \frac{emk_B T}{2\pi^2 \hbar^3} \int_0^\infty dE D(E, U) \ln \frac{1 + \exp[(E_F - E)/k_B T]}{1 + \exp[(E_F - E - eU)/k_B T]}, \quad (1)$$

where k_B is the Boltzmann constant, $\hbar = h/2\pi$, h is the Planck constant, e is the charge of the carrier (an electron here), m is its effective mass, E is its energy, T is the temperature, E_F is the Fermi level, U is the external potential (bias), and $D(E)$ is the energy-dependent transmission rate. The quantity $D(E)$ is expressed via the rates of transparency for the depletion region, $D_s(E)$, and that for the DBRTS, $D_r(E)$. If the tunnellings through the DBRTS and the SB are incoherent (i.e., statistically uncorrelated), $D(E)$ is equal to the product $D_s D_r$. This approximation is correct when the mean free path of an electron (l) in the semiconductor is less than the width of the depletion region. We note here the fact that the electrons with resonant energies $E_r < 0.1\text{eV}$ only, take part in tunnelling in the structure considered. These are energies of the order of the lowest resonant level in the DBRTS for typical parameters. The dependence of the mean free path (l) on the concentration (n_0) of doped shallow impurities, at $T = 300\text{K}$, are shown in the Fig. 2. This dependence is calculated using the data on the electron mobility for various E_r [6].

The dependence of the width of the depletion region L_S on n_0 , $L_S = \sqrt{\frac{\varepsilon_S \phi(0)}{2\pi e^2 n_0}}$, is also shown in this figure using typical values of the dielectric permittivity, $\varepsilon_S = 10.4$ (GaAs), and the height of the potential barrier at the interface $\phi(0) = 0.6\text{eV}$. We note from the Fig. 2 that the transmission of the electrons have to be coherent in the concentration domain of $10^{17}\text{cm}^{-3} < n_0 < 10^{19}\text{cm}^{-3}$.

According to this, we must, in fact, consider the process of the resonant tunnelling in the three-barrier (two-well) structure in our case. Quantitative characteristics of this process are strongly dependent on the details of the potential structure given. We should emphasize here that the Schottky approximation, widely used for the description of the potential profile (homogeneously smeared positive charges with concentration n_0), is improper for $n_0 \geq 10^{18}\text{cm}^{-3}$, because the width of the Schottky layer becomes comparable with the distances between the impurity centres, $a = n_0^{-1/3}$. For this reason, we have justified the model description of a potential in a depletion region, based on the solution of the Poisson equation,

$$\nabla^2 \phi(\mathbf{r}) = -\frac{4\pi e^2}{\varepsilon_S} n(\mathbf{r}) \theta(\phi), \quad (2)$$

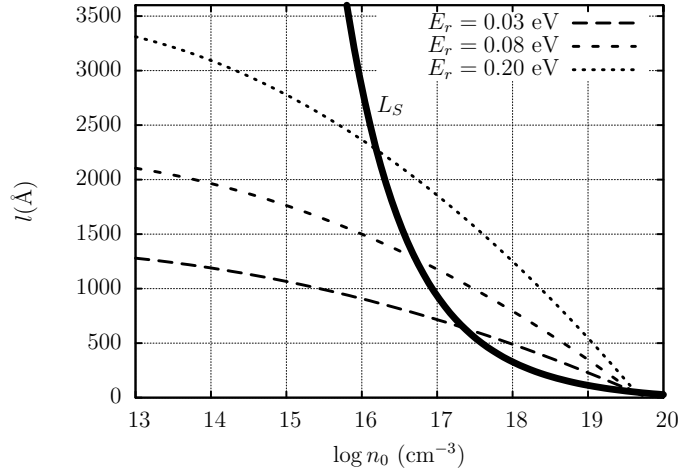


Fig. 2. Dependence of the mean free path (l), as well as the width of the depletion region (L_S), on the concentration (n_0) of shallow doping impurities.

with the boundary conditions:

$$\phi(\mathbf{r})|_{x=0} \equiv \phi(0) = \phi_0 - eU, \quad (3a)$$

$$\phi(\mathbf{r})|_L = \nabla_n \phi(\mathbf{r})|_L = 0, \quad (3b)$$

where ϕ_0 is the height of the potential in the depletion region at zero bias ($U = 0$) and $L(y, z)$ is the surface defined by the Eq. (3b). The space distribution of the positive charges has been modelled as follows: the “smeared” unit charges are placed on the sites of a cubic lattice with the period $a = n_0^{-1/3}$ and the volume $\Omega = (aN)^3$, N being the number of lattice points in each direction (x, y, z). Mathematically stated,

$$n(\mathbf{r}) = \sum_{\mathbf{l}} (\gamma/\pi)^{3/2} \exp(-\gamma(\mathbf{r} - a\mathbf{l})^2), \quad l_x, l_y, l_z = \overline{0 \dots N}. \quad (4)$$

The approximate solution of the Eq. (2), with the boundary conditions (3), was obtained by using the procedure of minimization of the variational functional, shown below, with a trial function satisfying the boundary conditions in Eq. (3):

$$\phi(\mathbf{r}) = \phi(0) \left[1 - \frac{x}{L(y, z)} \right]^2, \quad L(y, z) = \sqrt{\frac{\varepsilon_s \phi(0)}{2\pi e^2}} \left[n_0 + \nu \sum_{\lambda} e^{-\mu(\rho - a\lambda)^2} \right]^{-1/2}. \quad (5)$$

Here $\rho = (y, z)$, $\lambda = (l_y, l_z)$, and μ, ν are the variational parameters. The calculated spatial potential profile, with the built-in DBRTS in the depletion region,

$$\Phi(x, 0, z) \Big|_{x \geq 0} = \phi(\mathbf{r}) \Big|_{z=0} + V_0 \left[\theta(x - x_1)\theta(x_2 - x) + \theta(x - x_3)\theta(x_4 - x) \right] \quad (6)$$

is shown in the Fig. 3, for the following values of the parameters: $\phi(0) = 0.6$ eV, $n_0 = 4 \times 10^{18} \text{ cm}^{-3}$, $\gamma = 6.3 \times 10^{12} \text{ cm}^{-2}$ (these values define the reduction of the

“point” charge magnitude by ten times at a distance equal to the nearest centre), and $x_1 = 190\text{\AA}$ (the distance of the nearest barrier of the DBRTS from the metal-semiconductor interface. The DBRTS parameters are $x_2 - x_1 = x_4 - x_3 = 30\text{\AA}$ (barrier widths), $V_0 = 1\text{eV}$ (barrier height), and $x_3 - x_2 = 40\text{\AA}$ (quantum well width). The solid line in the Fig. 3, refers to the case $n(\mathbf{r}) = n_0$.

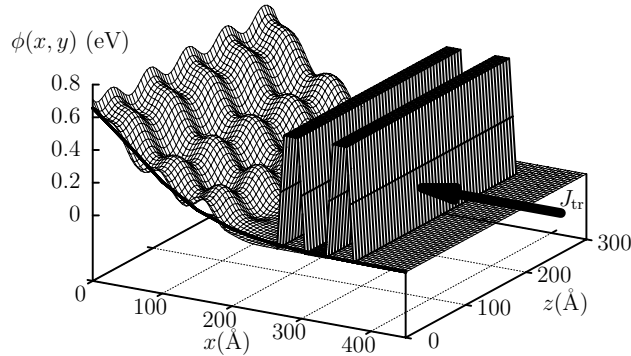


Fig. 3. The shape of a typical potential in the RTSC as a function of the coordinates x and z .

The calculation of the transmission rates $D(E)$ was carried out using the modified WKB procedure (e.g., see Ref. [7]). In accordance with the WKB approximation, the wave function of an electron in the region $x_j \leq x \leq x_{j+1}$ is of the form $\psi_j = A_j F_j$, where $A_j = \begin{pmatrix} a_j \\ b_j \end{pmatrix}$, $F_j = \begin{pmatrix} \phi_j^- \\ \phi_j^+ \end{pmatrix}$, $\phi_j^\pm(x) = |k_j(x)|^{-1/2} \exp \left[\pm \int_{\xi_{j-1}}^x k_j(x) dx \right]$, a_j, b_j are constants, $k_j(x) = \sqrt{2m_j(\Phi(x) - E)}$, m_j is the effective mass in the region j , and $\Phi(x)$ is the potential profile of the structure considered. We have $\xi_j = x_j$ for the case of the barriers with vertical walls. The matrices A_j , which refer to the neighbouring regions, are connected to each other by $A_{j+1} = G_j M_j N_j$, where

$$\begin{aligned}
 G_j &= \begin{pmatrix} \frac{1}{2}g_j(1+g_j^2)e^{i(k_j-k_{j+1})x_j} & \frac{1}{2}g_j(1-g_j^2)e^{-i(k_j+k_{j+1})x_j} \\ \frac{1}{2}g_j(1-g_j^2)e^{i(k_j+k_{j+1})x_j} & \frac{1}{2}g_j(1+g_j^2)e^{-i(k_j-k_{j+1})x_j} \end{pmatrix}, \\
 g_j &= \left(\frac{m_{j+1}}{m_j} \right)^{1/4}, \quad M_j = \begin{pmatrix} e^{-\delta_j} & 0 \\ 0 & e^{\delta_j} \end{pmatrix}, \\
 N_j &= \begin{cases} T, & \text{when } \left. \frac{dU}{dx} \right|_{\xi_{j+1}} > 0 \\ T^+, & \text{when } \left. \frac{dU}{dx} \right|_{\xi_{j+1}} < 0 \end{cases}, \quad T = \begin{pmatrix} \frac{1}{2}e^{i\pi/4} & \frac{1}{2}e^{-i\pi/4} \\ e^{-i\pi/4} & e^{i\pi/4} \end{pmatrix}.
 \end{aligned} \tag{7}$$

Here $\delta_j = \int_{\xi_j}^{\xi_{j+1}} k_j(x) dx$, and we use the Jeffrey's transformations (e.g., see Ref. [8]) to write the matrix T . The matrices G_j were obtained from the condition of continuity of both the wave functions and the flux must be continuous at $x = x_j$. The rate of transparency is defined as

$$D = \left[\left(\prod_{j=1}^S G_j M_j N_j \right)_{11} \right]^{-2} \quad (8)$$

for a structure which incorporates a number of S interfaces. The result for the calculation of $D(E)$ is shown in the Fig. 4, for the same parameters as for Fig. 3, alongwith $\gamma = 0$ and $U = 0.1\text{eV}$. It is seen clearly that the main contribution to $D(E)$ is due to the first (lowest in energy) resonant level E_r which lies energetically close to the resonant level of the DBRTS.

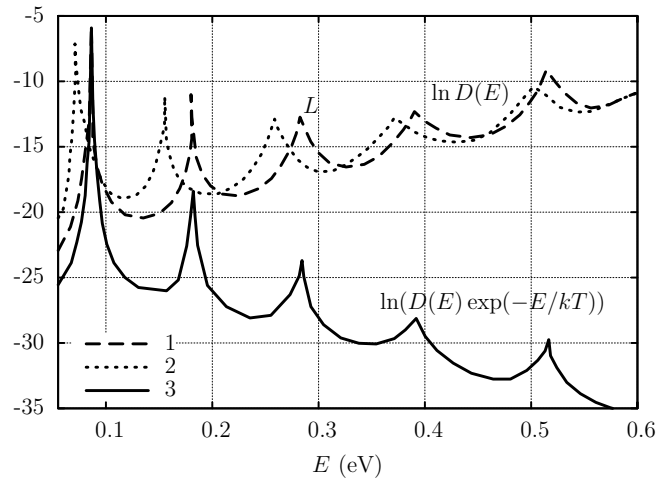


Fig. 4. The function $D(E)$ for two different values of n_0 : the curve 1 refers to the value $n_0 = 4 \times 10^{18} \text{cm}^{-3}$ and the curve 2 to $n_0 = 6 \times 10^{18} \text{cm}^{-3}$. The curve 3 describes the integrand in Eq. (1) at the room temperature ($T = 300\text{K}$).

The coordinate dependence of the depletion region $L(y, z)$, Eq. (5), results into a significant dependence of the transmission rates on the coordinates of the *percolation point* (y, z) on the surface described by Eq. (5). In the Fig. 5, we show the dependence of $D(E_r)$ on U for the minimum (at $y = z = a/2$, red curve) and the maximum (at $y = z = 0$, blue curve) respectively of $L(y, z)$. The green curve in this figure represents the surface-averaged [over $L(y, z)$] dependence of $D_{\text{ef}}(E)|_{E=E_r}$ on U . The black line refers to the case of incoherent tunnelling through all the barriers of the RTSC.

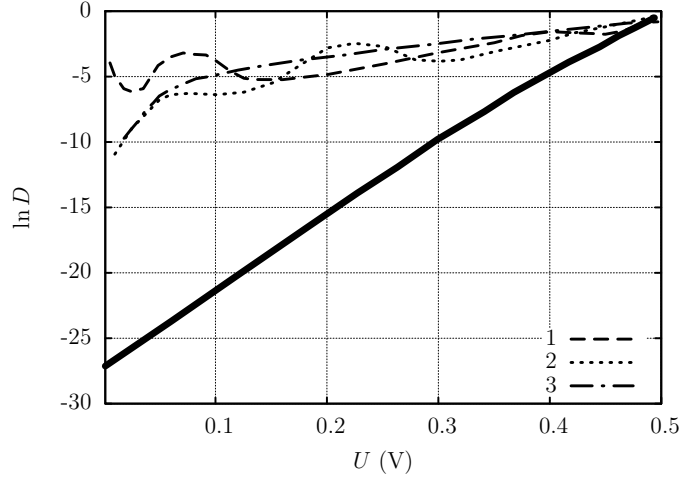


Fig. 5. Dependence of $\ln D(E_r)$ on U for the minimum (curve 1) and the maximum (curve 2) values of L . The curve 3 represents the surface $[L(y, z)]$ -averaged dependence of $\ln D(E_r)$ on U . The solid line refers to the case of incoherent tunnelling of electrons through all the barriers of the RTSC.

To evaluate the current we have to determine the quantity $\Phi(x)$, which consists of the two terms: the potential of the depletion region $\phi(x, U)$ and the potential energy of the DBRTS. The first one is defined as the solution of the Poisson equation, see Eq. (2),

$$\Delta\phi = -\frac{4\pi e}{\varepsilon_s}\rho(x), \quad \rho = \begin{cases} en_0, & 0 < x < x_1, \quad x_4 < x < L, \\ 0 & x_1 < x < x_4, \quad x > L. \end{cases} \quad (9)$$

with the usual boundary conditions for the depletion region of width L [cf. Eq.(3)]

$$\phi(0, U) = \phi(0, 0) + \epsilon U, \quad \phi(L, U) = \left. \frac{\partial\phi(x, U)}{\partial x} \right|_{x=L} = 0. \quad (10)$$

As a result, one obtains

$$\begin{aligned} \phi(x, U) = & \frac{2\pi n_0 N e^2}{\varepsilon_s} (x - L)^2 \\ & + \frac{2\pi n_0 N e^2}{\varepsilon_s} \begin{cases} (x_4 - x_1)(2x - x_4 - x_1), & 0 < x < x_1 \\ -(x - x_4)^2, & x_1 < x < x_4, \\ 0 & x_4 < x < L \end{cases} \end{aligned} \quad (11)$$

$$L^2 = \frac{\phi(0, U)\varepsilon_s}{2\pi e^2} + (x_4^2 - x_1^2). \quad (12)$$

The values $U > 0$ refer to the forward bias (the DBRTS is located in the coordinate interval $x_1 < x < x_4$). The field intensity in this interval is defined as:

$$F = -\frac{4\pi n_0 e}{\varepsilon_S} (L - x_4). \quad (13)$$

The quantity $D_s(E)$ necessary for evaluating the current is determined as a transparency of the barrier with the potential energy in Eq. (11), plus the potential energy associated with the image forces $\phi_{\text{im}} = -e^2/(4\epsilon_s x)$. In the interval of energies close to the top of the resulting barrier, where the coordinate dependence has the parabolic form, the transparency coefficient is of the following form:

$$D_s(E) \approx \frac{1}{1 + \exp[(\bar{\phi} - E)/E_0]}, \quad (14)$$

where $\bar{\phi} = \phi(0, U) - 1/(2\beta^2)$, $\beta = \{\epsilon_s/[4F(0)]\}^{1/4}$, $E_0 = \frac{\hbar\epsilon_s}{2\pi\sqrt{2m_s}\beta^3e^2}$, $F(0) = -e^{-1} \left. \frac{\partial\varphi(x, U)}{\partial x} \right|_{x=0}$. Note that $D_s(E)$ in Eq. (14) is a θ -like function with a half-width $\Gamma = \ln(3 + 2\sqrt{2})E_r$, which may be expressed via the quantities δ_j . Evaluation of the current-voltage characteristics (IVC) using the above formula yields the following expression

$$j_r \approx \frac{m\Gamma D_1 D_2}{\pi^{3/2}(D_1 + D_2)^2} \left[1 - \exp\left(-\frac{eV}{k_B T}\right) \right] \exp\left[\frac{E_F - E_1}{k_B T} + \left(\frac{\Gamma}{4k_B T}\right)^2\right] \times \text{erfc}\left\{\frac{2}{\Gamma}\left[\phi(0) - E_1 + \frac{\Gamma^2}{8k_B T}\right]\right\}, \quad (15)$$

where Γ is the half-width of the resonant level, and D_1 , D_2 are the transmission rates for the DBRTS barriers (the explicit forms of the quantities Γ , D_1 and D_2 are somewhat cumbersome, and hence omitted here). This expression is proper for the forward bias as well as for the reverse one.

The Fig. 6 demonstrates both the branches of the IVC for the following set of parameters at the room temperature ($T = 300\text{K}$: the DBRTS parameters the same as mentioned above, $m_s = 0.067m_0$, $m_b = 0.1m_0$, $n_0 = 10^{17}\text{cm}^{-3}$ and for four different values of x_1 (the distance between the DBRTS and the metal interface). The IVC's calculated (using the standard procedure) and shown in the Fig. 6 include not only the resonant-tunnelling current but also the over-barrier part of the current. Some regions with negative differential resistance (or, conductance) are observed in the back-biased branch of the IVC. The nature of these regions is obvious: they appear due to the blocking of the resonant-tunnelling current by the top part of the SB at voltages below a certain voltage $U_c < 0$. We would like to emphasize that the peak to valley ratio is of order of $10^2 \div 10^3$ in a wide range of parameters involved in the DBRTS.

Let us consider the forward branch of the IVC. The plotted functions are completely consistent with the assumptions made in this paper as to the character of the $I - V$ curves. At voltages U less than U_c , the currents in the investigated RTSC structure are relatively small. Then, in the vicinity of $U = U_c$, there is a precipitous rise in the current. For example, the current increases by approximately a factor of ten in response to a voltage change of 0.01eV . One is also struck by the large values of the parameter $\alpha = d \ln j / dU$, describing the differential steepness of the

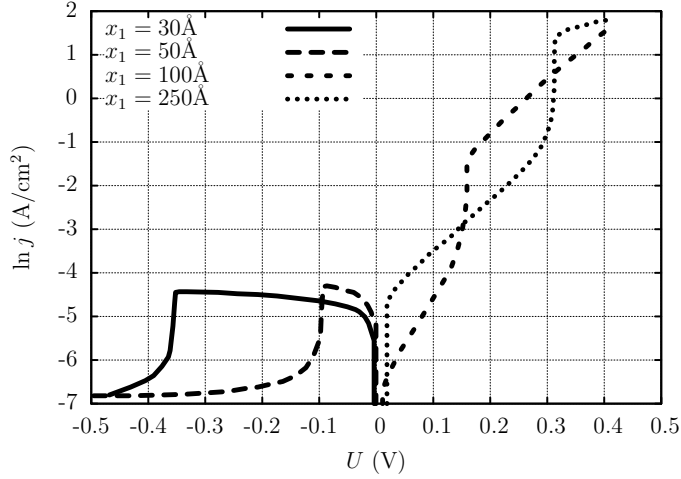


Fig. 6. The current-voltage ($I - V$) characteristics of the RTSC for the direct and the reverse bias, for four different values of x_1 (the metal to DBRTS distance).

IVC. They are much greater than the values of $e/k_B T$, typical for Schottky barriers (see Fig. 7). The values of U_c and α depend on many parameters of the structure; namely, the height of the SB, the dopant concentration, the geometric parameters of the DBRTS and its distance from the metal interface, etc.

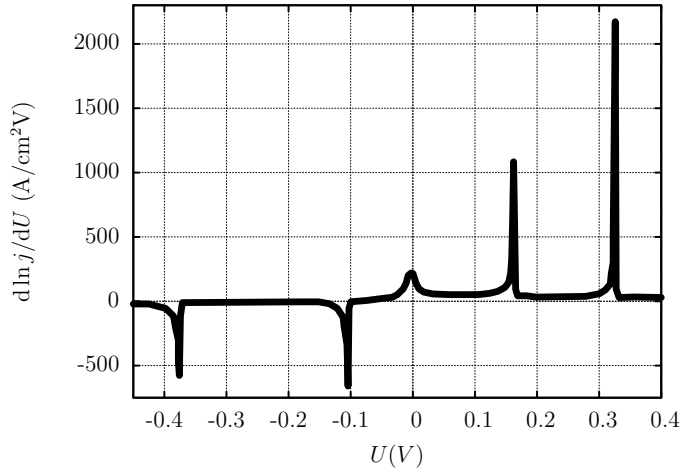


Fig. 7. The dependence of the differential steepness parameter of the IVC, $\alpha = d \ln j / dU$, at $T = 300\text{K}$, for the same values of the DBRTS parameters and four values of x_1 (the metal to DBRTS distance), the same as in the Fig. 6.

To explain the substantial growth of the current as the distance L from the metal

to the DBRTS is increased, it is convenient to refer to the Fig. 1. We see that at large L , the opening of the channel for the resonant tunnelling current (resonant energy E_r) occurs at a higher voltage $U = U_c$, which corresponds to a lower barrier height $\phi(x = 0, U)$. Consequently, the distribution function makes for higher currents in this case.

Finally, we should say a few words about the possible advantages of the system investigated here from the standpoint of practical applications. We note first that it retains the advantage that motivated the proposal made in the Refs. [4, 5] of replacing the conventional collector of the standard resonant-tunnelling diode by a Schottky collector; thus using the possibility of reducing the emitter-collector capacitance. Here increasing the distance between the metal and the DBRTS leads not only to a decrease in capacitance but also to a simultaneous increase in the steepness of the IVC (see the Figs. 6 and 7).

In addition, it should be noted that possible devices using the IVC given above (e.g., switches, amplifiers, rectifiers etc.) should possess good characteristics not only at low temperatures but even around room temperatures (note that the curves in the Figs. 6 and 7, were calculated for $T = 300\text{K}$).

Acknowledgements

The work presented above, grew out of a bi-lateral Indo-Ukrainian collaboration during the recent past, under the auspices of the Ministry of Sciences, Government of Ukraine, and the Department of Science and Technology (DST), Government of India. The last four authors express their respect and indebtedness to the (late) first author, Professor Dmitri I. Sheka, for his insights in this area of physics and dedicate this last paper bearing his name, to the academic zeal that characterized his persona. We are also grateful to Denis D. Sheka for helping us with the manuscript.

References

1. A. J. North, E. H. Linfield, M. Y. Simmons, D. A. Ritchie, M. L. Leadbeater, J. H. Burroughes, C. L. Foden, and M. Pepper, *Phys. Rev. B* **57**, 1847 (1998), URL http://prola.aps.org/abstract/PRB/v57/i3/p1847_1.
2. K. Yoh and Y. Kitasho, *Physica B: Condensed Matter* **272**, 24 (1999), URL <http://www.sciencedirect.com/science/article/B6TVH-3Y4BRT9-8/2/ce716dd8857059399f24429d979780d3>.
3. S. K. Jung, C. K. Hyon, J. H. Park, S. W. Hwang, D. Ahn, M. H. Son, B. D. Min, Y. Kim, and E. K. Kim, *Applied Physics Letters* **75**, 1167 (1999), URL <http://link.aip.org/link/?APL/75/1167/1>.
4. Y. Konishi, S. T. Allen, M. Reddy, M. J. W. Rodwell, R. P. Smith, and J. Liu, *Solid-State Electronics* **36**, 1673 (1993), URL <http://www.sciencedirect.com/science/article/B6TY5-46VKSC9-PP/2/53a5203f3643399d8b41caa110230b5b>.

12 REFERENCES

5. R. Smith, S. Alien, M. Reddy, S. Martin, J. Liu, R. Muller, and M. Rodwell, IEEE Electron. Device Lett. **15**, 295 (1994), URL <http://dx.doi.org/10.1109/55.296221>.
6. S. Sze, ed., *Physics of Semiconductor Devices* (John Wiley & Sons Inc, New York, 2006).
7. V. N. Dobrovolsky, D. I. Sheka, and B. V. Chernyachuk, Surface Science **397**, 333 (1998), URL <http://www.sciencedirect.com/science/article/B6TVX-3YXJC1S-6H/2/955485bbc616b2903f40d3507a43b0cd>.
8. N. Fröman and P. O. Fröman, *JWKB approximation: contributions to the theory* (North-Holland Publ.Co., Amsterdam, 1965).